


RESEARCH ARTICLE

High-resolution projections of evapotranspiration and water availability for Europe under climate change

Ștefan Dezsi¹ | Marcel Mîndrescu² | Dănuț Petrea¹ | Praveen Kumar Rai³ | Andreas Hamann⁴ | Mărgărit-Mircea Nistor⁵ 

¹Faculty of Geography, University of Babeș-Bolyai, Cluj-Napoca, Romania

²Department of Geography, University of Suceava, Suceava, Romania

³Department of Geography, Institute of Science, Banaras Hindu University, Varanasi, India

⁴Department of Renewable Resources, University of Alberta, Edmonton, Alberta, Canada

⁵Department of Hydrogeology, Earthresearch Company, Cluj-Napoca, Romania

Correspondence

Mărgărit-Mircea Nistor, Department of Hydrogeology, Earthresearch Company, Cluj-Napoca, Romania. Current affiliation: School of Civil and Environmental Engineering, Nanyang Technological University, Singapore.
Email: margarit@ntu.edu.sg

Evapotranspiration plays an essential role in estimating water balance, runoff and effective precipitation. To determine historical and projected water availability for Europe, we contribute high-resolution (1 km) estimates of monthly and annual potential evapotranspiration (ET₀) and actual evapotranspiration (AET₀). In the ET₀ calculation, the monthly and annual heat index I and annual α parameter were estimated following the Thornthwaite method, and AET₀ was calculated using the Budyko approach. The variables were estimated for a climate normal period that largely precedes an anthropogenic warming signal (1961–1990), and for two CMIP5 multi-model future projections (2011–2040 and 2041–2070). We project widespread and relatively uniform ET₀ increases of around 50–100 mm by the 2020s and 75–125 mm by the 2050s for most of Europe. These values imply important changes that may affect runoff and groundwater recharge. AET₀ was identified as important driver of water availability with more regional variability. Spatial mapping of changes relative to the normal baseline imply that all except northern parts of Europe are vulnerable to water deficits, with pronounced decrease expected in southern Europe. We provide high-resolution maps and data as an important tool for future natural resources management and climate change mitigation planning.

KEYWORDS

actual evapotranspiration, climate change, Europe, high spatial resolution models, potential evapotranspiration, water availability

1 | INTRODUCTION

The effects of the climate change over the last several decades have begun to transform natural and managed hydrological systems. One of the most sensitive and most visible climate change impacts on hydrological systems is the retreat of glaciers (Haeberli *et al.*, 1999; Kargel *et al.*, 2005; Oerlemans, 2005; Shahgedanova *et al.*, 2005; Dong *et al.*, 2013; Xie *et al.*, 2013; Elfarrak *et al.*, 2014; Nistor and Petcu, 2015). Less visible aspects of hydrological processes and water resources are equally affected, however. Decreases of the water table, reduction of water resources, reduced spring discharge and reduced river flows have been documented in

many parts of the world over the last decades (Collins, 2008; Aguilera and Murillo, 2009; Hidalgo *et al.*, 2009; Piao *et al.*, 2010; Jiménez Cisneros *et al.*, 2014). Concerns over the negative impacts of climate change on groundwater and water resources specifically in Europe have been raised in several studies (Brouyère *et al.*, 2004; Yustres *et al.*, 2013; Čenčur Curk *et al.*, 2014; 2015; Kløve *et al.*, 2014; Právělie, 2014; Právělie *et al.*, 2014). Further contributing to negative impacts of climate change on groundwater quality are increases of groundwater temperature (Taylor and Stefan, 2009; Kløve *et al.*, 2014) and subsequent changes to chemical reactions that occur in soils (Figura *et al.*, 2011; Haldorson *et al.*, 2012; Kløve *et al.*, 2012).

Changes to evapotranspiration, measured as potential (ET₀) and actual evapotranspiration (AET₀), are expected to negatively influence the availability of water resources. Because the measures integrate both changes in temperature and precipitation to describe a primarily climate-driven water balance, they are especially relevant for agricultural systems (Allen, 2000; Gowda *et al.*, 2008; Gerrits *et al.*, 2009; Nistor and Porumb-Ghiurco, 2015). The ET₀ and AET₀ metrics have been used in regional-scale to subcontinental-scale studies to track historical changes to the water balance, and for assessment of risks to food production and water resource availability (e.g., Chen *et al.*, 2006; Gao *et al.*, 2007; Gao *et al.*, 2012; Kousari *et al.*, 2013). In Europe, Nistor *et al.* (2016), Nistor *et al.* (2017a; 2017b) and Ambas and Baltas (2012) document historical increases of evapotranspiration, as well as potential climate change impacts. Kurnik *et al.* (2015) estimate soil water deficits for agricultural regions in Europe based on actual evapotranspiration. ET₀ and AET₀ metrics have become an indispensable indicator and measure of climate driven changes to water balance. The metrics also serve as the basis for risk assessments for agricultural systems and the development of mitigation strategies, for example by planning where investments in irrigation systems may become necessary. The metrics are further useful for surface water and groundwater modelling and other types of hydrogeology studies.

In this paper we contribute high-resolution estimates of potential and actual evapotranspiration, covering the full extent of Europe, using methodologies that we have

previously developed in smaller-scale studies (Nistor and Porumb-Ghiurco, 2015). We determine ET₀, AET₀ and water availability for a baseline historical reference period that has good weather station coverage and pre-dates a strong anthropogenic warming signal (the 1961–1990 climate normal period) as well as for two CMIP5 multi-model future projections for near-term planning (2011–2040) based on projections with only moderate uncertainties, as well as for longer-term planning (2041–2070).

2 | MATERIALS AND METHODS

2.1 | Study area

The study area is diverse with respect to climate, physical aspects, agricultural systems and other land use activities. The area analysed in this study extends from Crete Island in the south to Scandinavian Peninsula in the north and from Atlantic Ocean in the west including also the British Isles to east Europe plain up to 66°42' longitude east (Figure 1). Mean annual temperatures for the baseline period range from approximately –14 to +19 °C (Figure 2a) mean annual precipitation ranges from just over 200 mm to almost 3,700 mm (Figure 2d). The projected changes from a CMIP5 ensemble model for the 2020s (2011–2040 projection) and 2050s (2041–2070) that are the basis for this analysis are also shown for reference in Figure 2. Climatologies include extreme cold conditions in the Alps with altitudes reaching 4,800 m, cool maritime conditions in the north,

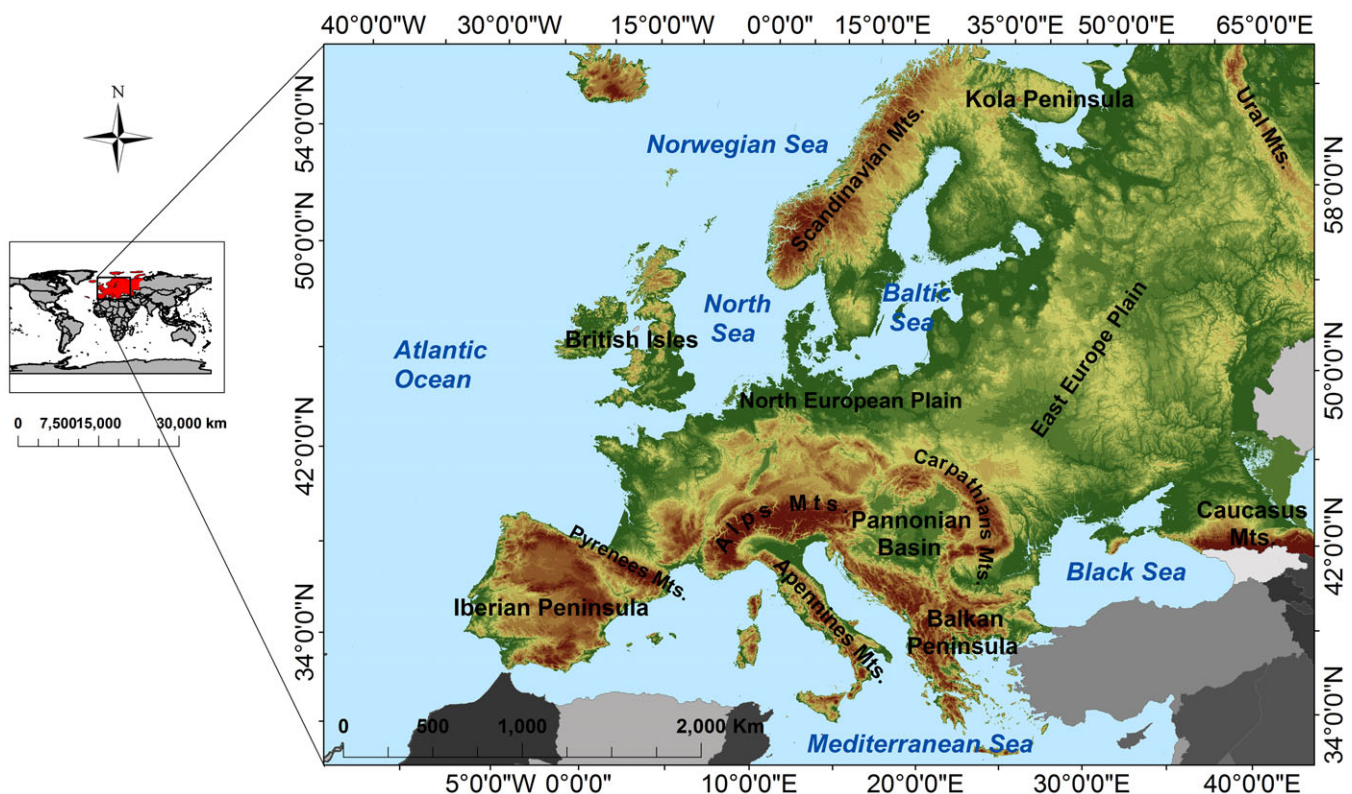


FIGURE 1 Study area with topography and regional names as used in the text for reference [Colour figure can be viewed at wileyonlinelibrary.com]

Saharan and Mediterranean influences in the south, continental climates in the east and oceanic influence in the west. The minimum values of precipitation are found in the south-east Europe and in the south of the Iberian Peninsula while the highest values are found in the mountain areas of Alps, Dinaric and Scandinavian Mountains. According to Kottek *et al.* (2006), the central, north central, south and some territories from the southeastern parts of the Europe has Cfa climate, which implies the warm temperate climate with hot summer and fully humid period during 1 year. In the eastern and the southeastern sides of the study area there are Dfa and Dfb climates that denote a generally cool climate with relatively warm summers. In the northeast parts of Europe and in the Scandinavian Peninsula the climate is classified as cool including the summers (Dfc class). Oceanic climates with warm summers are found north of the Iberian Peninsula (Csb), and with hot summers and little precipitation in the south of the Iberian Peninsula (Csa).

2.2 | Climate data and future projections

High-resolution gridded surfaces at 1 km cell size were developed in an Albers Equal Area Conic projection for Europe. Potential and actual evapotranspiration are based on monthly temperature and precipitation at the same resolution and projection for the 1961–1990 baseline period. Future projections were developed with the delta method based on multi-model CMIP5 projections for the 2011–2040 and 2041–2070 periods (hereafter referred to as 2020s and 2050s). The baseline reference data for monthly precipitation were constructed with the on parameter regression of independent slopes model (PRISM) by Daly

et al. (2006), while monthly temperature surfaces are based on the ANUSPLIN interpolation method following Mitchell and Jones (2005).

Future projections represent an ensemble average of 15 AOGCMs of the CMIP5 multi-model data set, corresponding to the IPCC Assessment Report 5 (Intergovernmental Panel on Climate Change, 2013). The individual models were chosen to represent major clusters of similar AOGCMs (Knutti *et al.*, 2013) that had high-validation statistics in their CMIP3 equivalents (Scherrer, 2011). The models are CanESM2, ACCESS1.0, IPSL-CM5A-MR, MIROC5, MPI-ESM-LR, CCSM4, HadGEM2-ES, CNRM-CM5, CSIRO Mk 3.6, GFDL-CM3, INM-CM4, MRI-CGCM3, MIROC-ESM, CESM1-CAM5 and GISS-E2R. We selected a median emission scenario, represented by the representative concentration pathway (RCP) 4.5 that globally predicts a +1.4 °C (± 0.5) by the 2050s.

The low-resolution AOGCM projections for the 2020s and 2050s were expressed as deviation from the reference normal period, using the historical AOGCM output provided at a monthly temporal resolution for the 1961–1990 period. Temperature values from AOGCMs were converted to anomalies (or delta values) in °C for temperature or % for precipitation relative to 1961–1990 period. The low-resolution anomalies were then overlaid on the high-resolution (1 km) temperature and precipitation reference grids to arrive at the final gridded surfaces that form the basis for ET₀ and AET₀ calculations for the future periods. To avoid step artefacts at the boundaries of low-resolution AOGCM grid cells, we apply bilinear interpolation to the anomaly grids prior to overlay. Since our projection periods have low temporal resolution (30-year averages for monthly

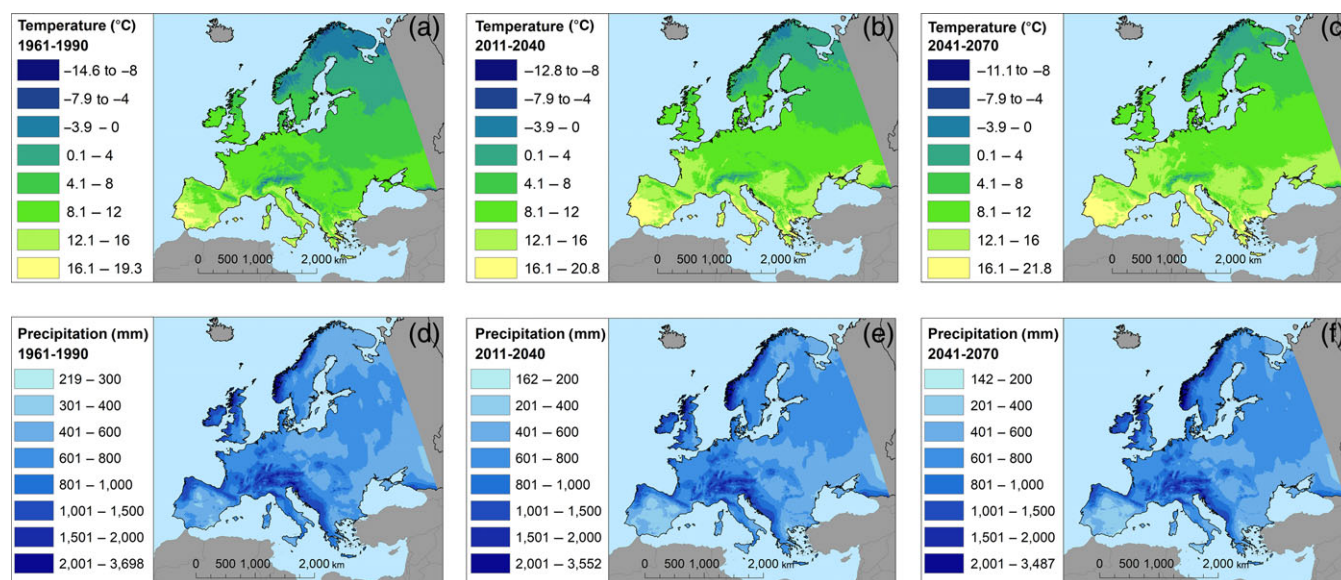


FIGURE 2 Mean annual temperature (a–c) and mean annual precipitation (d–f) for the historical reference period from 1961 to 1990 (a, d), for a near-term multi-model CMIP5 climate change projection for the 2020s (b, e) and for a medium-term projection for the 2050s (c, f). Monthly and annual climate grids for these periods form the basis for subsequent evapotranspiration and water availability estimates [Colour figure can be viewed at wileyonlinelibrary.com]

temperature and precipitation), we do not require temporal downscaling or bias correction of AOGCMs. Further information on the methodological details for precipitation and temperature grids are provided by Wang *et al.* (2006) and Wang *et al.* (2016).

2.3 | Potential evapotranspiration

We are using Thornthwaite's (1948) method to calculate monthly potential evapotranspiration data (ET₀). This metric is widely used in hydrology and agricultural studies (Zhao *et al.*, 2013; Čenčur Curk *et al.*, 2014; Cheval *et al.*, 2017). Grids of ET₀ were calculated from 1-km resolution average monthly temperature grids for current and projected future periods as described in the previous section according to the following formula:

$$ET_0 = 16 \left(\frac{10T_i}{I} \right)^\alpha, \quad (1)$$

where ET₀ is the monthly potential evapotranspiration (mm), T_i is the average monthly temperature (°C), ET₀ = 0 if $\bar{T}_m < 0$, I is the heat index (Equation 2) and α is the complex function of heat index (Equation 3).

$$I = \sum_{i=1}^{12} \left(\frac{T_i}{5} \right)^{1.514}, \quad (2)$$

where T_i is the monthly air temperature.

$$\alpha = 6.75 \times 10^{-7} I^3 - 7.71 \times 10^{-5} I^2 + 1.7912 \times 10^{-2} I + 0.49239, \quad (3)$$

where I is the annual heat index.

For negative values of temperature, we substitute a value of zero for the heat index I , where the values cannot be computed. The operations were implemented using the "Mosaic" function in ArcGIS (Figure S1, Supporting Information).

2.4 | Budyko equation for AET0 and water availability

The calculation of the annual AET₀ was performed following the Budyko approach. This method estimates if temperatures are high enough to produce evaporation from the rainfall (Gerrits *et al.*, 2009). Specifically, we use the Budyko equation to integrate the annual data of ET₀ and annual precipitation for the three periods, for estimations of AET₀ for Europe. The AET metric is widely applied in hydrology, climatology and agriculture (Čenčur Curk *et al.*, 2014; Nistor and Porumb-Ghiurco, 2015) and is also relevant for water balance studies. For example, Roderick and Farquhar (2011) have used an adapted Budyko equation to estimate the changes in the water availability for catchment-scale studies in Australia. We estimated AET₀ according to

the Budyko equation (Equation 4) and also derive water availability (Equation 6) reported in units of mm/year,

$$\frac{AET_0}{Pa} = \left[\left(\varphi \tan \frac{1}{\varphi} \right) (1 - \exp^{-\varphi}) \right]^{0.5}, \quad (4)$$

where AET₀ is the actual land cover evapotranspiration (mm), Pa is the total annual precipitation (mm) and φ is the aridity index (Equation 5).

$$\varphi = \frac{ET_0}{Pa}, \quad (5)$$

$$\text{Water availability} = Pa - AET_0. \quad (6)$$

All calculations were implemented using the ArcGIS environment (<http://esri.com>).

3 | RESULTS

3.1 | Current and projected heat indices for Europe

The annual heat index I varies from 0 to 95 in the historical reference period, from 0 to 107 for 2020s projections and from 0 to 114 in the future (Figure 3). High values of annual heat index (above 80) for all three periods were appear in the western parts of Europe, especially in the Iberian Peninsula, but also along the costal line of Italy and in the south of Greece. Low values of annual heat index (below 10) were found in the Alps Range, in the Scandinavian and in the Carpathian Mountains. Low values were identified also in the north of Great Britain and in the east of Europe, near the Black Sea, just north to the Caucasus Mountains. Substantial spatial shifts in the heat index I are apparent throughout the entire study region. A breakdown of heat index values by months is provided as Figures S2–S4 and the α parameter is shown in Figure S5 for the reference normal period (1961–1990), and two projections (2020s and 2050s), respectively.

3.2 | Monthly and annual potential evapotranspiration

Annual ET₀ shift throughout the study are with the maximum value for the historical reference period increasing to 1,031 mm for the 2020s and 1,130 mm for the 2050s (Figure 4). The baseline map of ET₀ (Figure 4a) shows the high values of ET₀ in the south, southeast and west of the Europe while the lower values extends in the Alps, Dinaric, Carpathians and Scandinavian Mountains. In the near- and medium-term future, the high values of ET₀ are expected in the west, south and south central sides of the Europe, with values up to 500 mm in the most of the territory (Figure 4b,c). The absolute changes maps between present and future projections are shown (Figure 8a,b), indicating in which regions most of the changes to annual ET₀ are expected. The exposed regions to high positive changes in the annual ET₀ are located

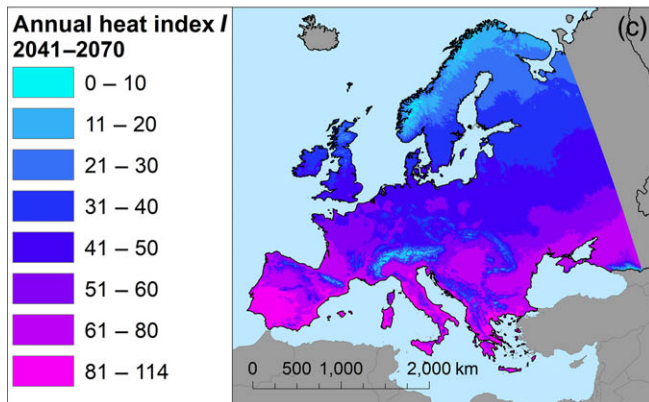
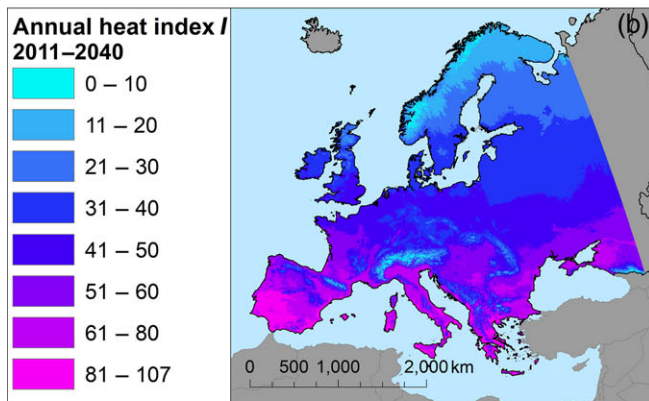
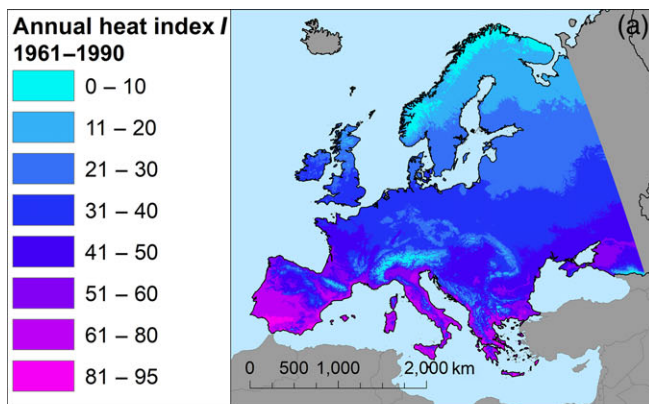


FIGURE 3 Annual heat index (I) for the 1961–1990 reference period (a), a multi-model CMIP5 climate change projection for the 2020s (b) and projections for the 2050s (c). Figures S2 and S3 provide a monthly breakdown of this annual index [Colour figure can be viewed at wileyonlinelibrary.com]

mainly in the west, south and southeast of Europe. Some places with significant negative changes (-100 mm) are also found in the north of Europe, in the Scandinavian Peninsula and in the Alps Range.

Changes to monthly potential evapotranspiration values (ET₀) are expected to change more severely in the summer months than in the winter months in response to climate change (compare January and July values across Figures S6–S8). The maximum changes to ET₀ values in response to climate change occur more in the west and

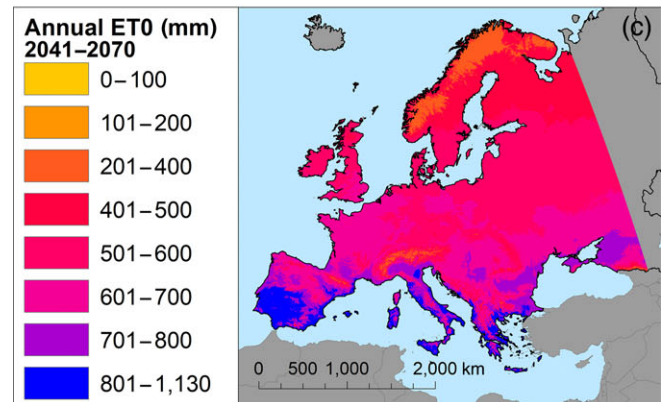
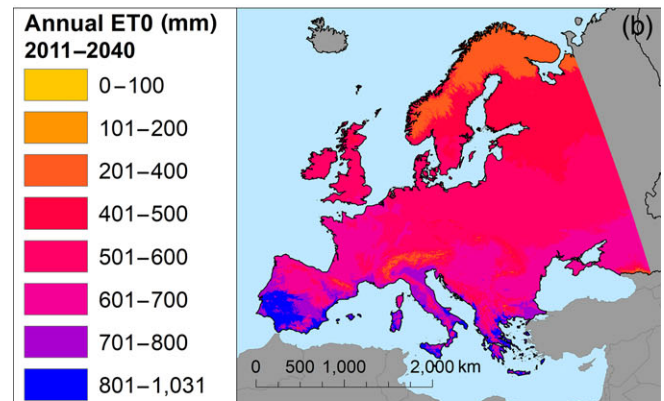
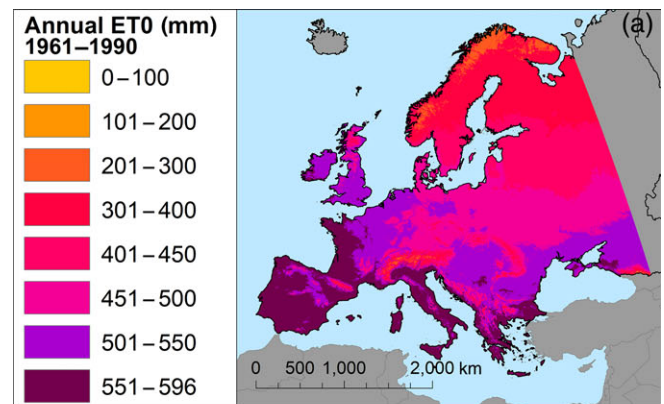


FIGURE 4 Annual potential evapotranspiration (ET₀) for the 1961–1990 reference period (a), a multi-model CMIP5 climate change projection for the 2020s (b) and projections for the 2050s (c). Figures S6–S8 provide a monthly breakdown of potential evapotranspiration [Colour figure can be viewed at wileyonlinelibrary.com]

south of the continent while the lower values belong to the winter months (January, February, respective December) and spread in the east and north of the continent.

3.3 | Actual evapotranspiration and water availability in Europe

Using the Budyko equation, and aridity index (ET₀/precipitation) was calculated as the basis for deriving AET₀ values for the Europe. The aridity index ranges from

0 to 2.7 for the reference period, with maximum values increasing to 5.6 and 6.7 for the near- and medium-term future, respectively (Figure 5), registering the high values in the central and south of the Iberian Peninsula, south of Italy including Sicily, south, east and northeast of Greece in both periods. Medium values of the aridity index (around 1.3–2) could be observed in the Pannonian basin, Mediterranean Islands, north of east of Romania, Black Sea and in the eastern sides of the Europe. Lower values of aridity index were depicted in the mountains areas, north of Europe, central and eastern sides of Europe, but also in the British Islands.

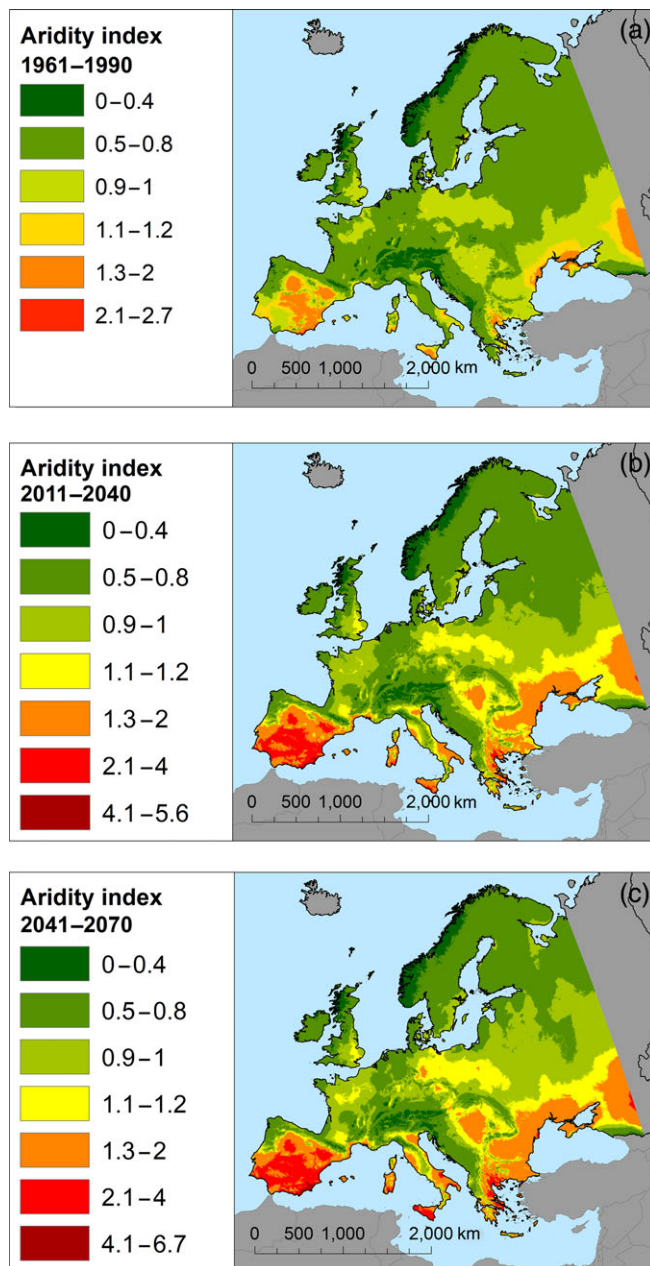


FIGURE 5 Aridity indices for the 1961–1990 reference period (a), a multi-model CMIP5 climate change projection for the 2020s (b) and projections for the 2050s (c) [Colour figure can be viewed at wileyonlinelibrary.com]

Figure 6 depicts the AET0 metric related to the three periods (1961–1990 normal, 2020s and 2050s). The AET0 values range from 180 to 540 mm for the normal period, from 161 to 724 mm for the 2020s projections and from 141 to 764 mm for the 2050s projections. Higher values (over 500 mm) of AET0 in all three periods are mainly located in the south of Europe, especially on the Dalmatian Coast of Adriatic Sea, in the west of Italian Peninsula, in north of Iberian Peninsula and south of France. The lower values of AET0 (below 200 mm) are located in the south of Iberian Peninsula, in the east and in the north of Europe in

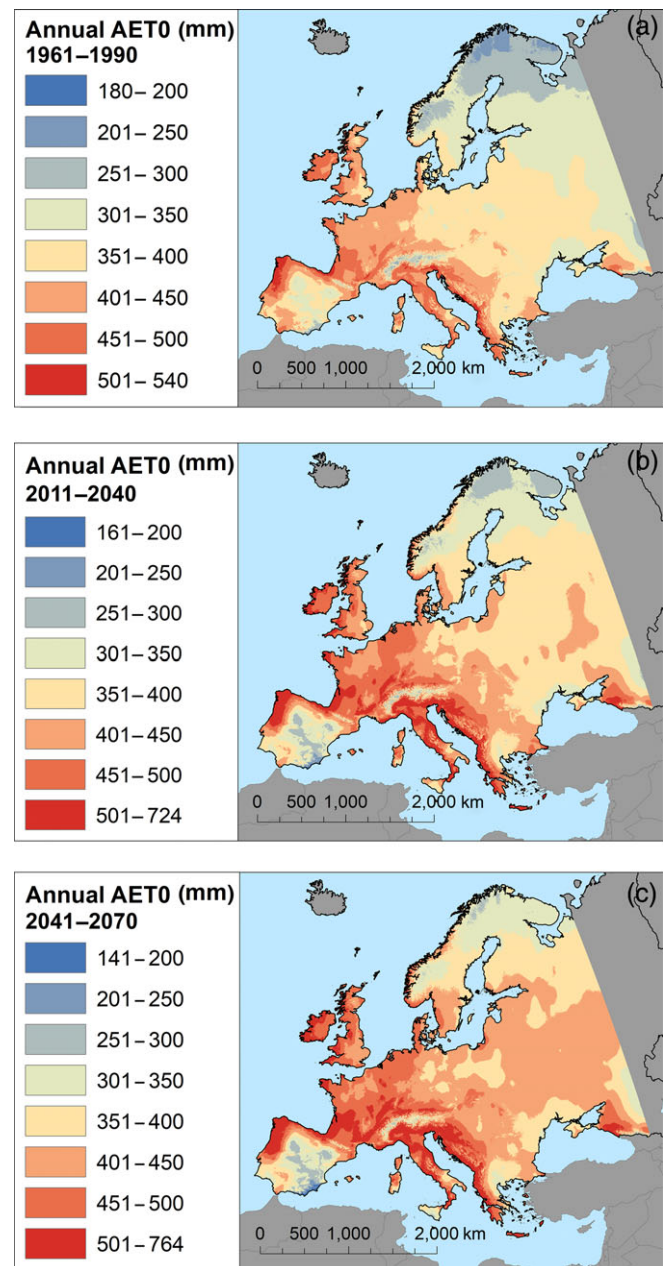


FIGURE 6 Annual actual evapotranspiration (AET0) for the 1961–1990 reference period (a), multi-model CMIP5 climate change projection for the 2020s (b) and projections for the 2050s (c) [Colour figure can be viewed at wileyonlinelibrary.com]

both periods. Regions with low AET₀ of Europe are also Sicily, Alps Range and south of continental Greece territory. Changes in the absolute values of AET₀ are shown in Figure 8c,d. The most striking changes are found in the Alps and Dinaric Mountains, in the eastern and northeastern sides of Europe. The maximum absolute changes reach 187 mm (reference climate versus 2020s).

Based on annual AET₀ and annual precipitation, we estimate the water availability for Europe (Figure 7). For the baseline, the water availability varies from 13 to 3,408 mm, indicating the high values (over 1,000 mm)

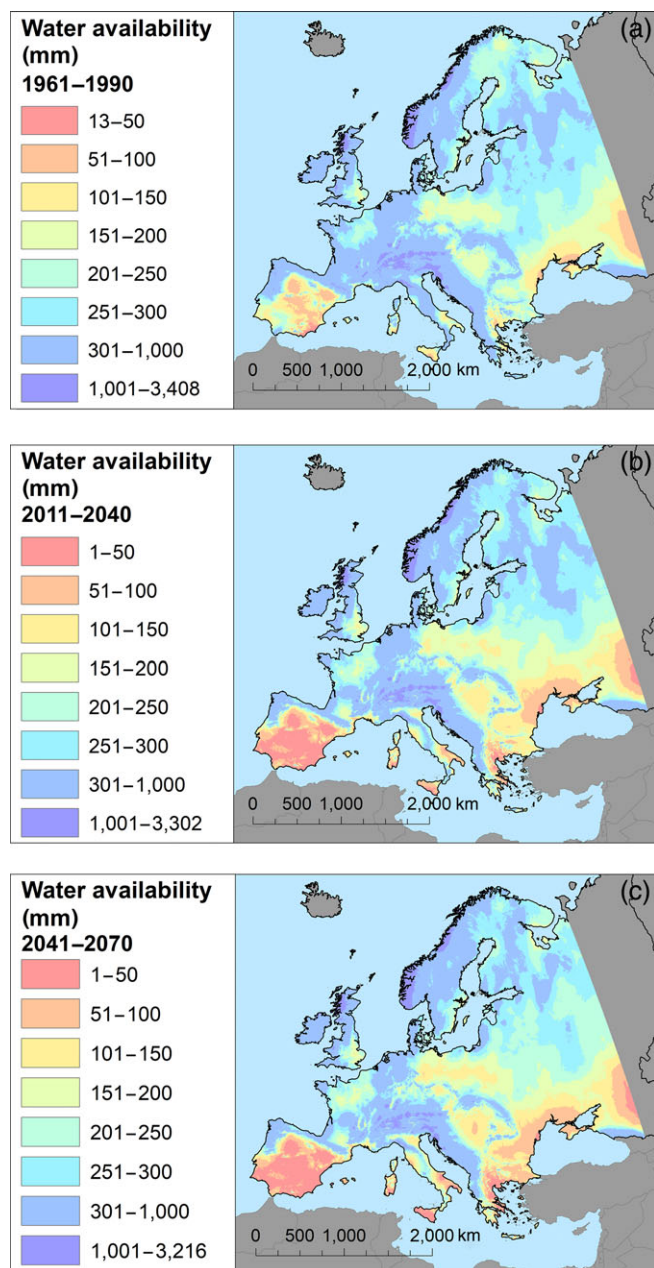


FIGURE 7 Annual water availability for the 1961–1990 reference period (a), a multi-model CMIP5 climate change projection for the 2020s (b) and projections for the 2050s (c) [Colour figure can be viewed at wileyonlinelibrary.com]

primarily in mountain areas. Regarding future projections, maximum values for water availability decrease to 3,302 mm (2020s) and 3,216 mm (2050s). The changes are most pronounced in the southern part of Europe, indicating the highest vulnerable to climate change (Figure 8e,f).

4 | DISCUSSION

Our analysis of the effect of climate change on the evapotranspiration and water availability of Europe has been carried out for near-term (2020s) and medium-term (2050s) projections. AOGCM outputs from different modelling groups conform well in the near-term, and they are also a very close match to observed climate trends over the last 20 years (Isaac-Renton *et al.*, 2014). Thus, our analysis of change from the 1970s to 2020s (observed 1961–1990 normal versus projected average 2011–2030) shown in Figure 8 should be very close to what managers and decision makers should use for climate change adaptation planning for the near-term future. While we provide 2050s data layers for medium-term planning, we should note that they come with larger uncertainties that we do not analyse in this study, and long-term planning (e.g., 2080s) would require a careful analysis of large uncertainties due to different AOGCMs and RCP scenarios (Wang *et al.*, 2016).

We find that the water availability in Europe is dependent not only on changes in evapotranspiration (ET₀), but also the projected precipitation regime turns out to be a major driver in the AET₀ calculation and water balance. Due to the projected trends in precipitation and AET₀ (Figure 8c,d), water availability is expected to be reduced throughout most of Europe, but spatial variability is high with the most pronounced decrease expected in southern Europe (Figure 8e,f). A notable result in terms of practical applications is the widespread annual ET₀ increase of around 50–100 mm by the 2020s and 75–125 mm by the 2050s, observed throughout central Europe (Figure 8a,b). These values imply important changes that may affect runoff and groundwater recharge. Such an increase of ET₀ would significantly affect agriculture through crop evapotranspiration, possibly requiring changes in crops or supplemental irrigation.

Our analysis for Europe generally conforms to previous regional studies. For example, estimates of ET₀ calculated by Čenčur Curk *et al.* (2014) in a study on groundwater resources in the southeast Europe, the ET₀ maximum values reaches 900 mm in the south of Italy and south of Greece for the present period (1991–2020) and around 1,040 mm for future period (2021–2050). Cheval *et al.* (2017) report annual ET₀ values which ranges from 300 to 800 mm in the southeast of Europe, and Nistor *et al.* (2016), using the CARPATCLIM database, find annual ET₀ values of 373 to 769 mm for the recent period (1991–2010) in the Carpathian region, very similar to values estimated here for the

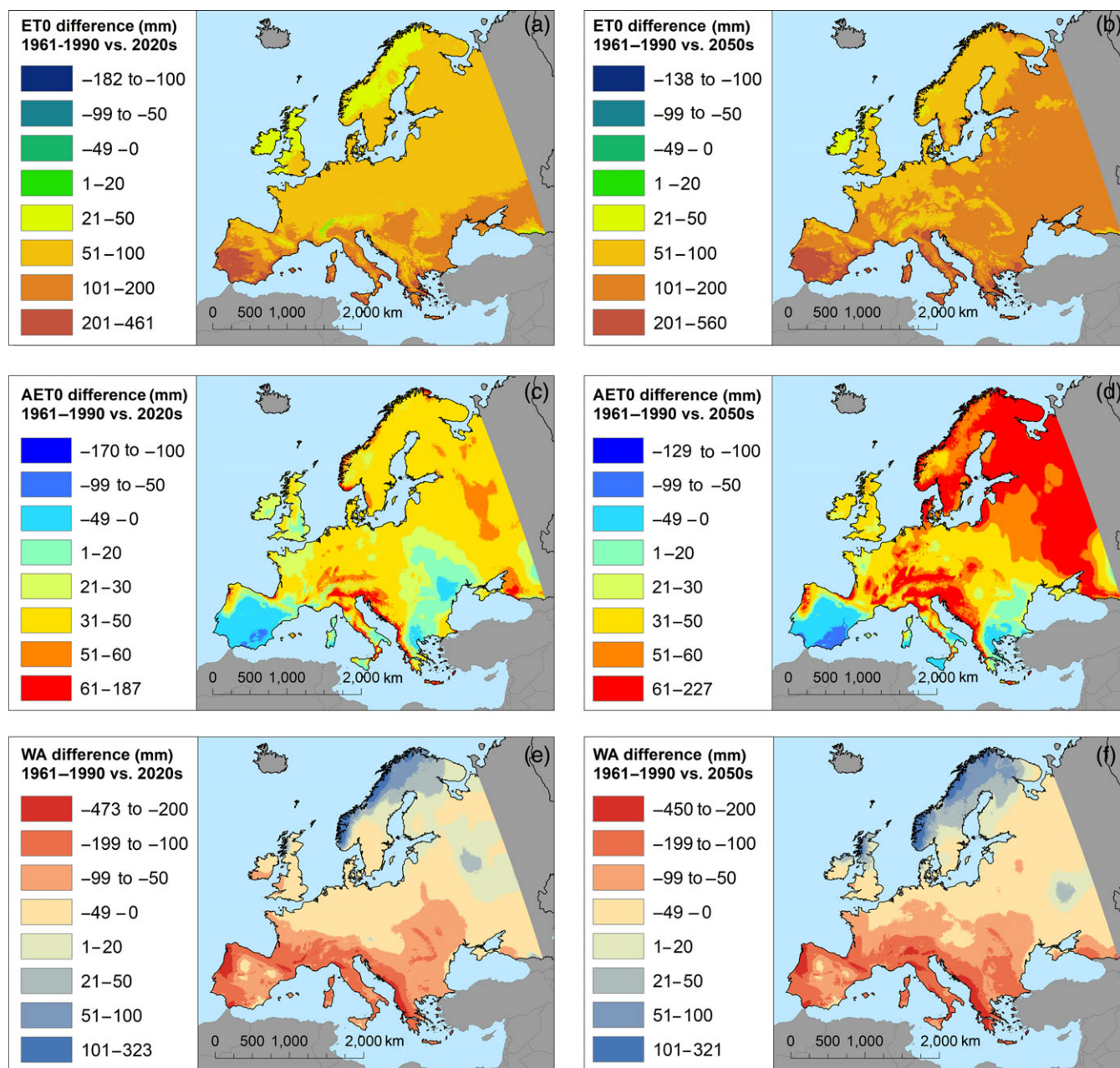


FIGURE 8 Absolute differences between the historical reference period and future projections for the 2020s and 2050s for potential evapotranspiration ET0 (a, b), actual evapotranspiration AET0 (c, d) and water availability WA (e, f) [Colour figure can be viewed at wileyonlinelibrary.com]

same region. Similar general concordance of ET0 values and geographic patterns were observed when comparing our data with a regional study for the Emilia-Romagna lowland of northern Italy (Nistor and Porumb-Ghiurco, 2015). Also, values of AET0 for different regions of Europe are in good agreement with the values of AET0 carried out using the Budyko approach by Čenčur Curk *et al.* (2014) for the southeast Europe and Nistor and Porumb-Ghiurco (2015) for the Emilia-Romagna region.

As a technical note, we should point out that for temperatures below 0 °C we assume no available energy for evapotranspiration. The representative annual heat index

I for present and future periods was calculated summing the monthly heat index I for the 12 months in which the zero values were added, primarily to mountainous regions, the Scandinavian Peninsula and northeastern sides of Europe. For the British Islands, only a small area of Scottish Mountains was affected by this calculation, which also causes the α parameter to register minimum values in the north of Europe and in the elevated areas. Further, the fall and winter seasons show large areas with low values of monthly ET0 because of low values of monthly heat index I and α parameter as consequences of low temperature data in this period.

In conclusion, we find substantial projected changes to ETO and AETO, resulting in all but the northern parts of Europe being vulnerable to water deficits, with pronounced decrease expected in southern Europe. The results should have practical relevance for planning of water use for industry and agriculture for the near- and medium-term future. For the regions, where vulnerabilities to climate change appear to be highest from this analysis, we recommend follow-up work to focus on crop evapotranspiration assessments and on groundwater resources in order to mitigate and analyse the climate change impact on environment patterns. To support development of climate change mitigation planning for water and natural resource management, we provide out gridded data layers through the an open access database (<https://doi.org/10.5281/zenodo.1044306>). The data may be used for large-scale regional planning as well as for local-scale applications by climatologists, hydrogeologists and policymakers for planning, zoning and delimitation of critical water areas in Europe.

ORCID

Mărgărit-Mircea Nistor  <http://orcid.org/0000-0001-9644-5853>

REFERENCES

- Aguilera, H. and Murillo, J.M. (2009) The effect of possible climate change on natural groundwater recharge based on a simple model: a study of four karstic aquifers in SE Spain. *Environmental Geology*, 57(5), 963–974.
- Allen, R.G. (2000) Using the FAO-56 dual crop coefficient method over an irrigated region as part of an evapotranspiration intercomparison study. *Journal of Hydrology*, 229, 27–41.
- Ambas, V.T. and Baltas, E. (2012) Sensitivity analysis of different evapotranspiration methods using a new sensitivity coefficient. *Global NEST Journal*, 14(3), 335–343.
- Brouyère, S., Carabin, G. and Dassargues, A. (2004) Climate change impacts on groundwater resources: modelled deficits in a chalky aquifer, Geer basin, Belgium. *Hydrogeology Journal*, 12, 123–134.
- Čenčur Curk, B., Cheval, S., Vrhovnik, P., Verbovšek, T., Herrnegger, M., Nachtnebel, H.P., Marjanović, P., Siegel, H., Gerhardt, E., Hochbichler, E., Koeck, R., Kuschnig, G., Senoner, T., Wesemann, J., Hochleitner, M., Žvab Rožič, P., Brenčič, M., Zupančič, N., Bračić Železnik, B., Perger, L., Tahy, A., Tornay, E.B., Simonffy, Z., Bogardi, I., Crăciunescu, A., Bilea, I. C., Vică, P., Onuțu, I., Panaitescu, C., Constandache, C., Bilanici, A., Dumitrescu, A., Baci, M., Breza, T., Marin, L., Draghici, C., Stoica, C., Bobeva, A., Trichkov, L., Pandeva, D., Spiridonov, V., Ilcheva, I., Nikolova, K., Balabanova, S., Soupilas, A., Thomas, S., Zambetoglou, K., Papatolios, K., Michailidis, S., Michalopoloy, C., Vafeiadis, M., Marcaccio, M., Errigo, D., Ferri, D., Zinoni, F., Corsini, A., Ronchetti, F., Nistor, M.M., Borgatti, L., Cervi, F., Petronici, F., Dimkić, D., Matic, B., Pejović, D., Lukić, V., Stefanović, M., Durić, D., Marjanović, M., Milovanović, M., Boreli-Zdravković, D., Mitrović, G., Milenković, N., Stevanović, Z. and Milanović, S. (2014) *CC-WARE mitigating vulnerability of water resources under climate change*, WP3—vulnerability of water resources in SEE (Report Version 5). Available at: <http://www.ccware.eu/output-documentation/output-wp3.html>.
- Čenčur Curk, B., Vrhovnik, P., Verbovšek, T., Dimkić, D., Marjanović, P., Tahy, A., Simonffy, Z., Corsini, A., Nistor, M.M., Cheval, S., Herrnegger, M., Nachtnebel, H.P. (2015) Vulnerability of water resources to climate change in south-east Europe. In: *AQUA 2015 42nd IAH Congress, The International Association of Hydrogeologists, Rome, Italy*. Available at: <https://www.aqua2015.com/downloads.php>.
- Chen, S.B., Liu, Y.F. and Thomas, A. (2006) Climatic change on the Tibetan Plateau: potential evapotranspiration trends from 1961 to 2000. *Climatic Change*, 76, 291–319.
- Cheval, S., Dumitrescu, A. and Barsan, M.V. (2017) Variability of the aridity in the south-eastern Europe over 1961–2050. *Catena*, 151, 74–86.
- Collins, D.N. (2008) Climatic warming, glacier recession and runoff from alpine basins after the Little Ice Age maximum. *Annals of Glaciology*, 48(1), 119–124.
- Daly, C., Halbleib, M., Smith, J.I., Gibson, W.P., Doggett, M.K., Taylor, G.H. and Curtis, J. (2006) Physiographically-sensitive mapping of temperature and precipitation across the conterminous United States. *International Journal of Climatology*, 28, 2031–2064.
- Dong, P., Wang, C. and Ding, J. (2013) Estimating glacier volume loss used remotely sensed images, digital elevation data, and GIS modelling. *International Journal of Remote Sensing*, 34(24), 8881–8892.
- Elfarrak, H., Hakdaoui, M. and Fikri, A. (2014) Development of vulnerability through the DRASTIC method and geographic information system (GIS) (case groundwater of Berrchid), Morocco. *Journal of Geographic Information System*, 6, 45–58.
- Figura, S., Livingstone, D.M., Hoehn, E. and Kipfer, R. (2011) Regime shift in groundwater temperature triggered by the Arctic oscillation. *Geophysical Research Letters*, 38, L23401.
- Gao, G., Chen, D., Xu, C.Y. and Simelton, E. (2007) Trend of estimated actual evapotranspiration over China during 1960–2002. *Journal of Geophysical Research*, 112, D11120.
- Gao, G., Xu, C.Y., Chen, D. and Singh, V.P. (2012) Spatial and temporal characteristics of actual evapotranspiration over Haihe River basin in China. *Stochastic Environmental Research and Risk Assessment*, 26, 655–669.
- Gerrits, A.M.J., Savenije, H.H.G., Veling, E.J.M. and Pfister, L. (2009) Analytical derivation of the Budyko curve based on rainfall characteristics and a simple evaporation model. *Water Resources Research*, 45, W04403. <https://doi.org/10.1029/2008WR007308>.
- Gowda, P.H., Chavez, J.L., Colaizzi, P.D., Evett, S.R., Howell, T.A. and Tolk, J.A. (2008) ET mapping for agricultural water management: present status and challenges. *Irrigation Science*, 26(3), 223–237.
- Haerberli, W.R., Frauenfelder, R., Hoelzle, M. and Maisch, M. (1999) On rates and acceleration trends of global glacier mass changes. *Geografiska Annaler, Series A, Physical Geography*, 81, 585–595.
- Haldorsen, S., Heim, M. and van der Ploeg, M. (2012) Impacts of climate change on groundwater in permafrost areas – case study from Svalbard, Norway. In: Treidel, H., Martin-Bordes, J.J. and Gurdak, J.J. (Eds.) *Climate Change Effects on Groundwater Resources: A Global Synthesis of Findings and Recommendations. International Association of Hydrogeologists (IAH) –International Contributions to Hydrogeology*. London: Taylor & Francis Publishing, pp. 323–340, 414 pp.
- Hidalgo, H.G., Das, T., Dettinger, M.D., Cayan, D.R., Pierce, D.W., Barnett, T. P., Bala, G., Mirin, A., Wood, A.W., Bonfils, C., Santer, B.D. and Nozawa, T. (2009) Detection and attribution of streamflow timing changes to climate change in the western United States. *Journal of Climate*, 22(13), 3838–3855.
- Intergovernmental Panel on Climate Change. (2013) Summary for policy-makers. In: Stocker, T.F., Qin, D., Plattner, G.-K., Tignor, M., Allen, S.K., Boschung, J., Nauels, A., Xia, Y., Bex, V. and Midgley, P.M. (Eds.) *Climate Change 2013: The Physical Science Basis. Contribution of Working Group I to the Fifth Assessment Report of the Intergovernmental Panel on Climate Change*. Cambridge; New York, NY: Cambridge University Press, 1308 pp.
- Isaac-Renton, M.G., Roberts, D.R., Hamann, A. and Spiecker, H. (2014) Douglas-fir plantations in Europe: a retrospective test of assisted migration to address climate change. *Global Change Biology*, 20, 2607–2617.
- Jiménez Cisneros, B.E., Oki, T., Arnell, N.W., Benito, G., Cogley, J.G., Döll, P., Jiang, T. and Mwakalila, S.S. (2014) Freshwater resources. In: Field, C.B., Barros, V.R., Dokken, D.J., Mach, K.J., Mastrandrea, M.D., Bilir, T.E., Chatterjee, M., Ebi, K.L., Estrada, Y.O., Genova, R.C., Girma, B., Kissel, E.S., Levy, A.N., MacCracken, S., Mastrandrea, P.R. and White, L.L. (Eds.) *Climate Change 2014: Impacts, Adaptation, and Vulnerability. Part A: Global and Sectoral Aspects. Contribution of Working Group II to the Fifth Assessment Report of the Intergovernmental Panel on Climate Change*. Cambridge; New York, NY: Cambridge University Press, pp. 229–269.

- Kargel, J.S., Abrams, M.J., Bishop, M.P., Bush, A., Hamilton, G., Jiskoot, H., Kääh, A., Kieffer, H.H., Lee, E.M., Paul, F., Rau, F., Raup, B., Shroder, J. F., Soltesz, D., Stainforth, S., Stearns, L. and Wessels, R. (2005) Multispectral imaging contributions to global land ice measurements from space. *Remote Sensing of Environment*, 99(1), 187–219.
- Kløve, B., Ala-aho, P., Okkonen, J. and Rossi, P. (2012) Possible effects of climate change on hydrogeological systems: results from research on esker aquifers in northern Finland. In: Treidel, H., Martin-Bordes, J.J. and Gurdak, J.J. (Eds.) *Climate Change Effects on Groundwater Resources: A Global Synthesis of Findings and Recommendations. International Association of Hydrogeologists (IAH) – International Contributions to Hydrogeology*. Boca Raton, FL: Taylor & Francis Publishing, pp. 305–322, 414 pp.
- Kløve, B., Ala-Aho, P., Bertrand, G., Gurdak, J.J., Kupfersberger, H., Kværner, J., Muotka, T., Mykrä, H., Preda, E., Rossi, P., Bertacchi Uvo, C., Velasco, C. and Pulido-Velazquez, M. (2014) Climate change impacts on groundwater and dependent ecosystems. *Journal of Hydrology*, 518, 250–266.
- Knutti, R., Masson, D. and Gettelman, A. (2013) Climate model genealogy: generation CMIP5 and how we got there. *Geophysical Research Letters*, 40, 1194–1199.
- Kottek, M., Grieser, J., Beck, C., Rudolf, B. and Rubel, F. (2006) World map of the Köppen–Geiger climate classification updated. *Meteorologische Zeitschrift*, 15(3), 259–263.
- Kousari, M.R., Zarch, M.A.A., Ahani, H. and Hakimelahi, H. (2013) A survey of temporal and spatial reference crop evapotranspiration trends in Iran from 1960 to 2005. *Climatic Change*, 120, 277–298.
- Kumik, B., Kajfež-Bogataj, L. and Horionc, S. (2015) An assessment of actual evapotranspiration and soil water deficit in agricultural regions in Europe. *International Journal of Climatology*, 35, 2451–2471.
- Mitchell, T.D. and Jones, P.D. (2005) An improved method of constructing a database of monthly climate observations and associated high-resolution grids. *International Journal of Climatology*, 25, 693–712.
- Nistor, M.M. and Petcu, M.I. (2015) Quantitative analysis of glaciers changes from Passage Canal based on GIS and satellite images, south Alaska, A survey of temporal and spatial reference crop evapotranspiration trends in Iran from 1960 to 2005. *Applied Ecology and Environmental Research*, 13(2), 535–549.
- Nistor, M.M. and Porumb-Ghiurco, G.C. (2015) How to compute the land cover evapotranspiration at regional scale? A spatial approach of Emilia–Romagna region. *GEOREVIEW Scientific Annals of Ștefan cel Mare University of Suceava. Geography Series*, 25(1), 38–54.
- Nistor, M.M., Gualtieri, A.F., Cheval, S., Dezsi, S.T. and Boțan, V.E. (2016) Climate change effects on crop evapotranspiration in the Carpathian region from 1961 to 2010. *Meteorological Applications*, 23, 462–469.
- Nistor, M.M., Ronchetti, F., Corsini, A., Cheval, S., Dumitrescu, A., Rai, P.K., Petrea, D. and Dezsi, Ș. (2017a) Crop evapotranspiration variation under climate change in southeast Europe during 1991–2050. *Carpathian Journal of Earth and Environmental Sciences*, 12(2), 571–582.
- Nistor, M.M., Cheval, S., Gualtieri, A., Dumitrescu, A., Boțan, V.E., Berni, A., Hognogi, G., Irimuș, I.A. and Porumb-Ghiurco, C.G. (2017b) Crop evapotranspiration assessment under climate change in the Pannonian basin during 1991–2050. *Meteorological Applications*, 24, 84–91.
- Oerlemans, J. (2005) Extracting a climate signal from 169 glacier records. *Science*, 308, 675–677.
- Piao, S., Ciais, P., Huang, Y., Shen, Z., Peng, S., Li, J., Zhou, L., Liu, H., Ma, Y., Ding, Y., Friedlingstein, P., Liu, C., Tan, K., Yu, Y., Zhang, T. and Fang, J. (2010) The impacts of climate change on water resources and agriculture in China. *Nature*, 467(7311), 43–51.
- Prävălie, R. (2014) Analysis of temperature, precipitation and potential evapotranspiration trends in southern Oltenia in the context of climate change. *Geographia Technica*, 9(2), 68–84.
- Prävălie, R., Sîrodov, I. and Peptenatu, D. (2014) Detecting climate change effects on forest ecosystems in southwestern Romania using Landsat TM NDVI data. *Journal of Geographical Sciences*, 24, 815–832.
- Roderick, M.L. and Farquhar, G.D. (2011) A simple framework for relating variations in runoff to variations in climatic conditions and catchment properties. *Water Resources Research*, 47, W00G07. <https://doi.org/10.1029/2010WR009826>.
- Scherrer, S.C. (2011) Present-day interannual variability of surface climate in CMIP3 models and its relation to future warming. *International Journal of Climatology*, 31, 1518–1529.
- Shahgedanova, M., Stokes, C.R., Gurney, S.D. and Popovnin, V. (2005) Interactions between mass balance, atmospheric circulation, and recent climate change on the Djankuat Glacier, Caucasus Mountains, Russia. *Journal of Geophysical Research*, 110, D16107.
- Taylor, C.A. and Stefan, H.G. (2009) Shallow groundwater temperature response to climate change and urbanization. *Journal of Hydrology*, 375(3–4), 601–612.
- Thornthwaite, C.W. (1948) An approach toward a rational classification of climate. *Geographical Review*, 38, 55–94.
- Wang, T., Hamann, A., Spittlehouse, D.L. and Aitken, S.N. (2006) Development of scale-free climate data for western Canada for use in resource management. *International Journal of Climatology*, 26, 383–397.
- Wang, T., Hamann, A., Spittlehouse, D.L. and Carroll, C. (2016) Locally down-scaled and spatially customizable climate data for historical and future periods for North America. *PLoS One*, 11, e0156720.
- Xie, X., Li, Y.X., Li, R., Zhang, Y., Huo, Y., Bao, Y. and Shen, S. (2013) Hyperspectral characteristics and growth monitoring of rice (*Oryza sativa*) under asymmetric warming. *International Journal of Remote Sensing*, 34(23), 8449–8462.
- Yustres, Á., Navarro, V., Asensio, L., Candel, M. and García, B. (2013) Groundwater resources in the Upper Guadiana Basin (Spain): a regional modelling analysis. *Hydrogeology Journal*, 21, 1129–1146.
- Zhao, L., Xia, J., Xu, C., Wang, Z., Sobkowiak, L. and Long, C. (2013) Evapotranspiration estimation methods in hydrological models. *Journal of Geographical Sciences*, 23(2), 359–369.

SUPPORTING INFORMATION

Additional Supporting Information may be found online in the supporting information tab for this article.

How to cite this article: Dezsi Ș, Mîndrescu M, Petrea D, Rai PK, Hamann A, Nistor M-M. High-resolution projections of evapotranspiration and water availability for Europe under climate change. *Int J Climatol*. 2018;38:3832–3841. <https://doi.org/10.1002/joc.5537>